

Symmetry-Selective Observation of the N 1s Shape Resonance in N₂

U. Hergenhahn,^{*,†,‡} O. Kugeler,^{†,‡} A. Rüdel,[†] E. E. Rennie,^{†,‡} and A. M. Bradshaw[‡]

Fritz-Haber-Institut der Max-Planck-Gesellschaft, Faradayweg 4–6, 14195 Berlin, Germany, and Max-Planck-Institut für Plasmaphysik, Boltzmannstrasse 2, 85748 Garching, Germany

Received: October 19, 2000; In Final Form: March 23, 2001

Inner-shell photoelectron spectra of the N 1s level in N₂ have been measured with sufficient resolution to resolve the splitting between the gerade and ungerade components. The selective enhancement of the gerade component on the N₂ σ shape resonance is clearly seen, confirming that the resonant behavior is mainly caused by the σ_u channel. The splitting of the two components is found to be 97(3) meV.

Introduction

The N 1s- σ shape resonance in N₂ is a showcase example for inner-shell photoionization continuum resonances. Such resonances, which have been found in the photoabsorption spectra of a large number of molecules,^{1,2} can best be explained in terms of an interaction between the photoemitted electron and the surroundings of the photoemitter in the molecule. Because the molecule as a whole forms a potential well for the outgoing photoelectron, at certain energies resonant states can form, which have a strongly modified continuum wave function. This produces the continuum resonance. The symmetry and energy of this scattering state often resemble those of the lowest virtual (unoccupied) molecular orbital.³ Shape resonances have therefore often been described as the trapping of the outgoing electron in an antibonding molecular state, which subsequently decays into the molecular continuum. In the particular case of nitrogen, the N₂ 1s shape resonance corresponds to a trapping of the photoelectron in a $3\sigma_u^*$ orbital. Often, but not necessarily, the resonant state exhibits a nodal pattern that can be identified with a certain value of orbital angular momentum l . In this sense, the nitrogen shape resonance has been identified with an f -wave.

In nitrogen, four 1s atomic core electrons are available, from which two molecular orbitals of gerade and ungerade symmetry are formed. As the trapping state of the N₂ 1s shape resonance is of ungerade symmetry, from the dipole selection rules the resonance should appear only in the cross section of the N 1s σ_g component. The 1s σ_u component should not be influenced. This prediction, as well as the similarity of the resonant wave function to a $3\sigma_u^*$ antibonding orbital, was reported in early multiple scattering calculations.^{4–6} However, the symmetry selectivity of the resonance is difficult to observe experimentally. This is due to the fact that the energetic splitting between the 1σ gerade and ungerade states in N₂ is expected to be in the order of 100 meV, compared to an (average) N 1s ionization energy of 409.9 eV.⁷ Therefore, even in the high-resolution photoelectron spectra reported in the recent literature, the N 1s main line is seen only as a superposition of the σ_g and the σ_u components.⁸

In this article we report new high-resolution measurements of the N 1s photoelectron main line. Employing a setup with a

total apparatus resolution of 55(5) meV, we were able to observe directly the splitting of the core level line, to determine its value, and to follow the intensity ratio of the two symmetry components in the photon energy region of the discrete double excitations and the shape resonance. The ungerade symmetry of the shape resonance is clearly revealed in our results. A reanalysis of the published spectra of Kempgens et al.⁸ shows that they are consistent with the new findings reported here.

Earlier experimental^{8,9} and theoretical^{4,5,10,11} work concentrated on describing the photon energy dependence of the total N 1s cross section and its β parameter. The main problem posed to theory for a long time was the prediction of the correct energy position and the magnitude of the shape resonance. To some extent it was solved by Wilhelmy and Rösch,¹² as discussed below. Experimentally, two groups succeeded in demonstrating the σ character of the resonance using symmetry-resolved ion yield spectroscopy.^{13,14} The next step forward was the investigation of N 1s photoionization from fixed-in-space N₂ molecules.¹⁵ Pavlychev et al.¹⁶ considered the inversion symmetry of this experimental photoelectron angular distribution at the photon energy of the shape resonance and concluded that the original gerade/ungerade symmetry, or the delocalized character, of the core state is preserved in the photoemission process. This is consistent with resonant X-ray scattering experiments on O₂.¹⁷ The most recent calculations reported by Cherepkov et al.¹⁸ and Lin and Lucchese¹⁹ included continuum channel coupling for the first time, and the former has quantitatively reproduced the angular distribution measurements in ref 15.

Evidence showing that the shape resonance is of ungerade symmetry was recently found in K–V X-ray detection,²⁰ where the authors concluded from an amplification of the ungerade final valence hole states on the shape resonance that an enlarged population of 1s σ_g hole states is produced at this energy.²¹ A gerade/ungerade splitting of ca. 105 meV in the C 1s main line of the isoelectronic molecule ethyne (HCCH) was observed in photoionization spectra.²² The photon energy dependence of the intensity ratio of the two components measured soon afterward by Thomas et al.²³ showed a selective enhancement of the $1\sigma_g$ component, thus indicating that the observed shape resonance in this system is predominantly of σ_u symmetry.

Experimental Details and Data Analysis

The experiment reported in this article was performed at the undulator beamline U49 of the recently opened third generation

* Corresponding author. E-mail: hergenhahn@fhi-berlin.mpg.de.

[†] Fritz-Haber-Institut der Max-Planck-Gesellschaft.

[‡] Max-Planck-Institut für Plasmaphysik.

synchrotron radiation source BESSY II (Berlin, Germany). The beamline is equipped with a spherical grating monochromator,²⁴ covering the energy range of 150 to well above 1000 eV. Using a 1200 l/mm grating, for a photon energy of 400 eV, a photon flux of $9 \times 10^{10}/(100 \text{ mAs})$ at an exit slit setting of 20 μm has been measured.²⁵ With the same setting we determined a photon energy resolution of $29 \pm 5 \text{ meV}$ from an ion yield scan over the N 1s – π^* resonance around 401 eV. A value of 115(4) meV for the lifetime broadening of the N 1s⁻¹ π^* excited state has been used.²⁶ The $\pm 5 \text{ meV}$ error bar in the resolution is mainly from the uncertainty in the latter figure, which has to be disentangled from the experimental spectrum by a fit procedure. Electrons were detected with a hemispherical analyzer (Scienta SES-200)²⁷ mounted within the dipole plane under 54.7° with respect to the electric field vector. The ionization volume was enclosed by a stainless steel gas cell, which included a photoelectron dump to prevent backscattered electrons from entering the analyzer, and electrodes to apply a compensation voltage along the sample volume.²⁸ The pressure within the gas cell was estimated to be $3 \times 10^{-3} \text{ mbar}$. A curved analyzer slit of 200 μm width and pass energies of 10 and 5 eV in the Scienta analyzer were used. The resulting analyzer resolution was estimated to be 48(8) meV from the total experimental resolution (see below).

The data were recorded in short sweeps, which were saved separately. Small shifts between the different sweeps were compensated for by shifting the respective scans by an integer number of steps. The spectra were then summed and subjected to a least-squares fit to determine the spectroscopical quantities of interest. We assumed two underlying lines exhibiting one vibrational progression each. For the line shape, we have used a Lorentzian form distorted by post collision interaction (PCI). An analytical parametrization of the resulting profile due to Kuchiev and Sheinerman^{29,30} was chosen. The resulting curves were convoluted by a Gaussian to account for experimental broadening. For the three data points at lowest kinetic energy, fits were also carried out using the PCI model of van der Straten et al.³¹ The latter model explicitly includes the time dependence of the velocity of the PCI inducer, which is decelerated after emission of the Auger electron. An upper limit to the photoelectron kinetic energy for this effect to be sizable is approximately $E_{\text{kin}}^{3/2} < 100\Gamma$ (Γ is lifetime broadening). Different assumptions about other aspects of the underlying line structure, such as shape of the experimental background and simplifications for the Franck–Condon factors, were tested for their effect on the final result.

To obtain an unbiased fit, the weights for the experimental data points were derived from the respective values of the fit curve.³² The following parameters were allowed to vary, but were restricted to identical values for all lines and spectra, respectively: Gaussian line broadening, lifetime broadening, splitting of the two main components, and vibrational energy. To reproduce the spectra, it was necessary to allow for different Franck–Condon factors for the vibrationally excited states of g and u symmetry. Restricting the FC factors to the linear coupling model³³ did not significantly change the results.

To check the consistency of our new results, one of the two series of N₂ N 1s spectra published by Kempgens et al.⁸ has been reanalyzed in a similar fashion. The reader is referred to the original publication for details of the data acquisition. In brief, a cylindrical mirror analyzer aligned along the photon beam recorded photoelectrons entering the analyzer at a backward scattering angle of 54.7° with respect to the beam. Light was provided by the spectroscopy beamline X1B of the

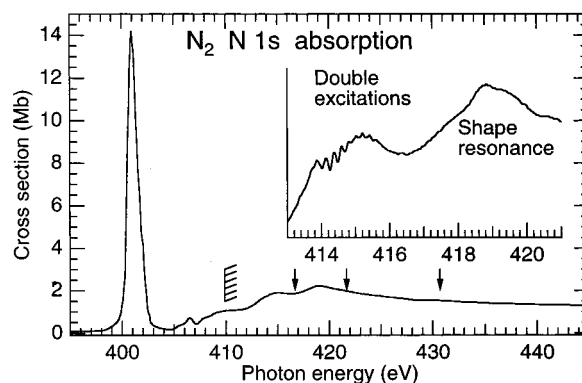


Figure 1. Nitrogen photoabsorption spectrum in the region of the N 1s ionization threshold and the shape resonance. Data are from Kempgens et al.⁸ and Chen et al.⁷ (inset). Arrows indicate the positions of the photoelectron spectra in Figure 2.

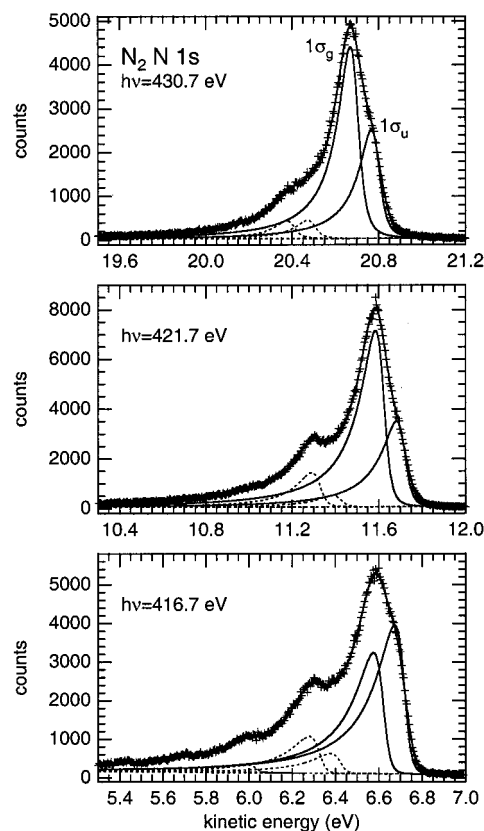


Figure 2. N 1s main line spectrum of N₂ recorded at three different photon energies. Solid lines indicate the final result of a least-squares fit and the results for the individual $v' = 0$ components before convolution by the apparatus profile. Broken lines denote $v' = 1$ and higher components.

National Synchrotron Light Source (Brookhaven, N.Y.). It turns out that results consistent with the analysis of the new spectra can be obtained, if in the least-squares fitting procedure the value of the lifetime broadening is fixed to a range consistent with the analysis of our new high-resolution spectra.

Results and Discussion

In Figure 1, for the purpose of illustration, published data for the nitrogen photoabsorption cross section are reproduced.⁸ Figure 2 shows N₂ N 1s main line spectra recorded at photon energies below (416.7 eV), at the maximum and above the shape resonance. In all spectra one observes that the line consists of two components, in particular, through the shoulder on the high

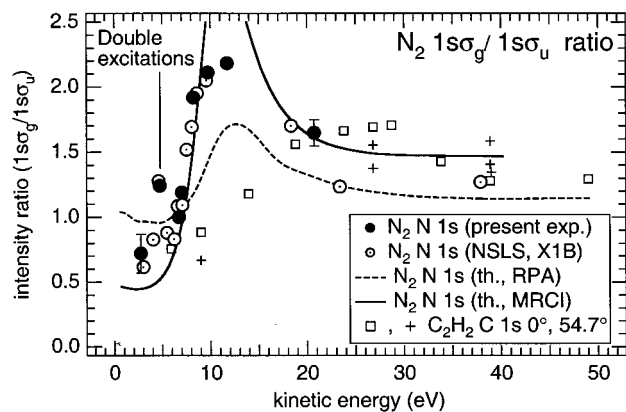


Figure 3. Photoionization intensity ratio into the two $N N_2 1s^{-1}$ molecular states. Broken and solid lines indicate theoretical results of Cherepkov et al.^{18,36} and Lin and Lucchese,¹⁹ which have been placed at an $N 1s$ ionization threshold of 409.9 eV.⁷ Results for the isoelectronic molecule ethyne from ref 23 are included for comparison.

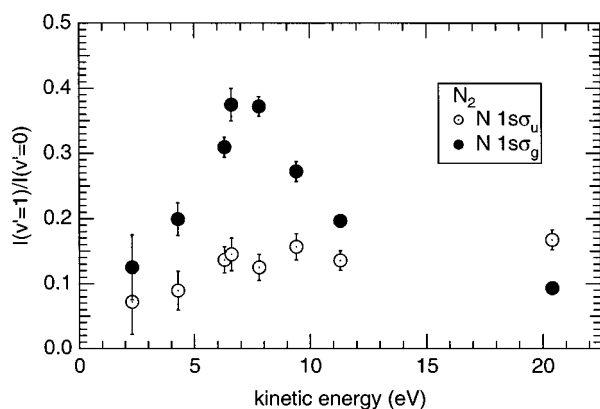


Figure 4. Intensity ratio of photoionization into the first vibrationally excited ($v' = 1$) and the vibrational ground state ($v' = 0$) of $N_2 1s^{-1}$.

energy flank of the peak. Quantitatively we have determined a splitting of 97(3) meV. Other results from the fit include a vibrational energy of 295(5) meV. This is smaller than the value of 314(4) meV given by Kempgens et al.,⁸ which can be explained by the neglect of the two-component nature of the $N 1s$ line in our previous work. The lifetime broadening can only approximately be given as 102(10) meV. A better estimate would require a detailed analysis of the intrinsic line shape of our analyzer, which is represented by a Gaussian to a good approximation.³⁴

The resulting intensity ratio $I(1\sigma_g)/I(1\sigma_u)$ is displayed in Figure 3. Two remarkable features can be seen immediately: (1) the enhancement of the gerade component in the shape-resonance region around 10 eV kinetic energy and (2) the deviation of the cross section ratio from the asymptotically expected value of unity, which can be seen even at the highest measured energy. The jump in the ratio curve occurs in the same energy region as the increase in the total cross section in Figure 1. From that we can conclude that it is indeed the gerade component that is mainly amplified. Simultaneously, also the vibrational coupling constant for this component increases. The ratio of first excited to ground ionic state, $I(v' = 1)/(v' = 0)$, is displayed in Figure 4.

The error bars for the measured values of $I(1\sigma_g)/I(1\sigma_u)$ are mainly due to variations between results for different model assumptions in the least squares procedure and can be estimated as ± 0.15 for the lowest and ± 0.1 for the highest kinetic energy of the BESSY II data set. Under the assumption of a perfectly

valid fit model, error values of less than ± 0.05 would arise from statistical error theory.³⁵

Both features (1 and 2) are predicted qualitatively by recent calculations.^{18,19} In extension of the original publication of Cherepkov, data points including both $\epsilon\sigma$ and $\epsilon\pi$ continuum channels calculated within the reported formalism were at our disposal.³⁶ According to earlier calculations, the π -channels are similar in magnitude and are unstructured.⁵ We must then ask why, even in the asymptotic region, the two partial cross sections are not equal in value. Dehmer and Dill⁵ have predicted in their multiple-scattering calculations roughly equal magnitudes for both σ channels, modified by EXAFS-like oscillations of opposite phase dependent on the g or u symmetry of the partial wave for kinetic energies larger than approximately 100 eV.

While the influence of the shape resonance on the (g/u) ratio is not reproduced exactly in the two calculations, the ratio of the $1\sigma_g/1\sigma_u$ intensities calculated solely from the $\epsilon\sigma$ continuum channels as published in ref 18 matches the experimental curve perfectly. It cannot be excluded that this agreement is only accidental, but it may also be an indication that the discrepancies between experiment and theory are due to the (nonresonant) $\epsilon\pi$ continuum channels on which theoretical studies have not yet focused.

The peak in the (g/u) ratio at kinetic energies around 4.7 eV is in a region where the influence of discrete double excitations in the absorption spectrum is most prominent.^{7,8} Excitations into neutral doubly excited states have been discussed in studies by Neeb et al.,^{37,38} where the double excitations were observed by the appearance of additional lines of high kinetic energy resulting from spectator decay of these states. In contrast, we observe here the decay into the competing valence participator channel, in which one of the excited electrons fills the valence hole while the other is ejected. This can be seen as an indirect process leading to the same state as direct $1s$ photoionization. Calculated potential curves for a number of doubly excited states are given in our earlier paper.³⁸ These states can be subdivided into double valence excitations of principal configuration $1s^{-1}val^{-1}1\pi_g^2$ and valence + Rydberg excitations with a configuration of $1s^{-1}1\pi_u^{-1}1\pi_g^1ryd^1$. Among these, the excitation into the $1s\sigma_g^{-1}1\pi_u^{-1}1\pi_g^13s\sigma_g^1$ doubly excited state, at a calculated excitation energy of 5.12 eV with respect to the $N 1s$ ionization potential (409.9 eV), is nearest to the feature we observe at 4.7 eV kinetic energy. Excitation into this state, with subsequent valence participator decay, would lead to a selective enhancement of the $1s\sigma_g$ ionization cross section. However, we believe our kinetic energy scale to be accurate to within ± 100 meV, so that the agreement of the excitation energy with the calculated value is not completely satisfactory. We note that the atomic Auger decays that were used as a probe for double excitations by Neeb manifest themselves over a larger range of photon energies, from about 408–417 eV where no conspicuous features are seen in our (g/u) ratio. Due to the different probe Neeb et al. probably detected the dissociative states of $1s^{-1}val^{-1}1\pi_g^2$ type, which may decay to a lesser extent via valence participator processes. Further theoretical work on this topic is clearly required.

The (g/u) ratio in the $C 1s$ photoionization of ethyne (C_2H_2 , Figure 3) shows values equal to those of nitrogen within the experimental accuracy at the lowest and highest kinetic energies sampled. However, in the intermediate region, the enhancement of the gerade cross section by the σ shape resonance is much stronger in nitrogen. This confirms the findings of Kempgens et al.,³⁹ who showed that the actual single-particle character of

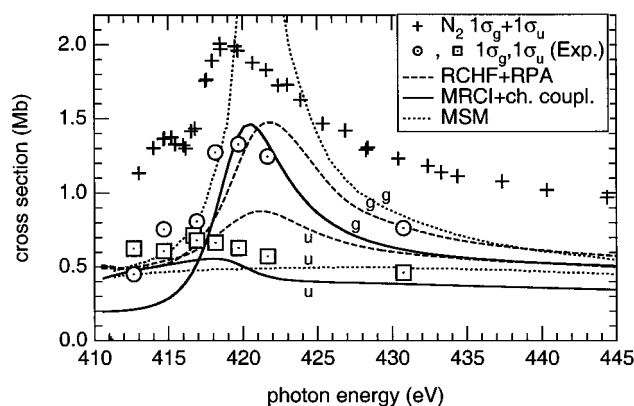


Figure 5. Cross section for ionization into the two N₂ molecular states. Crosses show the N₂ 1s⁻¹ partial cross section in absolute units,⁸ circles and squares are results for the two symmetry components from this work, and broken and solid lines indicate theoretical results of Cherepkov et al.¹⁸ (relaxed-core Hartree–Fock + random phase approximation) and Lin and Lucchese¹⁹ (multireference CI). Dotted lines are theoretical results of Dehmer and Dill⁵ (multiple-scattering model), which do not include g/u coupling.

the immediate post-threshold enhancement in ethyne is much smaller than the contribution from satellite channels. In a recent theoretical study on ethyne by Lin and Lucchese,⁴⁰ these results have been reproduced in essence. The main difference between N₂ and C₂H₂, with respect to the nature of the shape resonance, appears to lie in the lower threshold energy for satellite excitations in the C₂H₂ molecule. For example, for the triplet and singlet coupled π - π^* valence shake-up satellites (often designated S₁ and S₀), the energies relative to the 1s main line are 9.5 and 16.4 eV for N₂, but as low as 7.2 and 12.4 eV for C₂H₂.^{8,41}

Using the N 1s absolute ionization cross section from Kempgens et al.⁸ and the intensity ratio from this work, we can produce the 1 σ_g and 1 σ_u partial cross sections on an absolute scale. This has been done in Figure 5. This form of presentation allows a closer comparison with the theoretical results from refs 18 and 19. The ca. 1 Mb enhancement of the 1 σ_g cross section due to the resonance is, however, reproduced within the experimental accuracy. This represents a substantial progress compared to most of the earlier papers cited in the Introduction.⁸ Cherepkov¹⁸ et al. have essentially modified the dipole matrix element obtained from a relaxed-core Hartree–Fock (HF) calculation by solving for an improved matrix element within the random phase approximation (RPA). Their error in the position of the shape resonance, about 3 eV, therefore can be traced back to the underlying HF calculation, which is very similar to that of Lynch and McKoy.¹¹ These authors obtained a similar level of agreement.

The main point in the paper by Cherepkov¹⁸ was the prediction of interchannel coupling between g and u channels, which was excluded in earlier calculations. Because of that, the u channel has a smaller local maximum at the same energy as the g channel. This is however not identified in our data. The amount of coupling between g and u channels was again explored by Lin and Lucchese,¹⁹ but using a multireference configuration interaction calculation of the ground and ionic state as a starting point. The configuration basis included all single and double excitations into the first virtual π and σ orbitals as well as configurations with a single electron excited to a number of higher Rydberg orbitals. The results from this more complete approach suggest that the amount of g/u coupling is actually smaller, and the resulting cross section more similar to our experimental results than in the prediction of Cherepkov.

Moreover, a reduction of the importance of channel coupling when turning from a RCHF to a multiconfiguration description of the process could be demonstrated.^{19,40} The remaining effect of channel coupling on the 1 σ_u cross section can best be seen by comparison with the theoretical curve of Dill and Dehmer,⁵ for which the channels were not coupled. The too low cross sections for the 1 σ_g channel at low photon energies could result from the still incomplete inclusion of discrete double excitations.

Of the earlier papers, only the calculations of Wilhelmy and Rösch¹² seem to show an equally good overall agreement with experiment. Their so-called transition state potential (the potential resulting from a half-filled core hole) gives the correct position of the shape resonance at about 419 eV, although its use cannot be rigorously justified. On the other hand, the absolute magnitude of the cross section comes out too high in this work.

In conclusion, by using high-resolution undulator radiation from the BESSY II electron storage ring and a high-resolution electron spectrometer, we were able to resolve the inner shell photoelectron main line from N₂ into components of g and u symmetry. We have demonstrated directly the σ_u character of the N 1s shape resonance and have shown that it is considerably more intense than the C 1s shape resonance in C₂H₂ and C₆H₆, where satellite excitations contribute strongly to the cross section enhancement in the post-threshold region.^{23,42} On the contrary, in N₂ the shape resonance retains its single particle character. More generally, this paper shows how the unique qualities of third generation synchrotron radiation sources can be used for molecular spectroscopy.

Acknowledgment. Thanks are due to F. Bernal for help in data acquisition. We are grateful to R. R. Lucchese for making his results available prior to publication and to N. A. Cherepkov for sending an extended data set of his results in numerical form. The experiments at BESSY II were greatly helped by the enthusiastic support of a number of staff members, especially F. Senf. Part of this work has been funded by the Deutsche Forschungsgemeinschaft and by the Fonds der Chemischen Industrie. The National Synchrotron Light Source at Brookhaven National Laboratory is supported by the U.S. Department of Energy, Division of Material Sciences and Division of Chemical Sciences.

References and Notes

- (1) Sette, F.; Stöhr, J.; Hitchcock, A. P. *J. Chem. Phys.* **1984**, *81*, 4906–4914.
- (2) Nenner, I.; Morin P. In *VUV and soft X-ray photoionization studies*; Plenum Press: New York, 1996.
- (3) Sheehy, J. A.; Gil, T. J.; Winstead, C. L.; Farren, R. E.; Langhoff, P. W. *J. Chem. Phys.* **1989**, *91*, 1796–1812.
- (4) Dehmer, J. L.; Dill, D. *Phys. Rev. Lett.* **1975**, *35*, 213–215.
- (5) Dehmer, J. L.; Dill, D. *J. Chem. Phys.* **1976**, *65*, 5327–5334.
- (6) Loomba, D.; Wallace, S.; Dill, D.; Dehmer, J. L. *J. Chem. Phys.* **1981**, *75*, 4546–4552.
- (7) Chen, C. T.; Ma, Y.; Sette, F. *Phys. Rev. A* **1989**, *40*, R6737–R6740.
- (8) Kempgens, B.; Kivimäki, A.; Neeb, M.; Köppe, H. M.; Bradshaw, A. M.; Feldhaus, J. *J. Phys. B* **1996**, *29*, 5389–5402.
- (9) Lindle, D. W.; Truesdale, C. M.; Kobrin, P. H.; Ferrett, T. A.; Heimann, P. A.; Becker, U.; Kerkhoff, H. G.; Shirley, D. A. *J. Chem. Phys.* **1984**, *81*, 5375–5378.
- (10) Rescigno, T. N.; Langhoff, P. W. *Chem. Phys. Lett.* **1977**, *51*, 65–70.
- (11) Lynch, D. L.; McKoy, V. *Phys. Rev. A* **1984**, *30*, R1561–1564.
- (12) Wilhelmy, I.; Rösch, N. *Chem. Phys.* **1994**, *185*, 317–332.
- (13) Lee, K.; Kim, D. Y.; Ma, C. I.; Lapiano-Smith, D. A.; Hanson, D. M. *J. Chem. Phys.* **1990**, *93*, 7936–7945.
- (14) Shigemasa, E.; Ueda, K.; Sato, Y.; Sasaki, T.; Yagishita, A. *Phys. Rev. A* **1992**, *45*, 2915–2921.

- (15) Shigemasa, E.; Adachi, J.; Oura, M.; Yagishita, A. *Phys. Rev. Lett.* **1995**, *74*, 359–362.
- (16) Pavlychev, A. A.; Fominykh, N. G.; Watanabe, N.; Soejima, K.; Shigemasa, E.; Yagishita, A. *Phys. Rev. Lett.* **1998**, *81*, 3623–3626.
- (17) Glans, P.; Gunnelin, K.; Skytt, P.; Guo, J.-H.; Wassdahl, N.; Nordgren, J.; Ågren, H.; Gel'mukhanov, F. K.; Warwick, T.; Rotenberg, E. *Phys. Rev. Lett.* **1996**, *76*, 2448–2251.
- (18) Cherepkov, N. A.; Semenov, S. K.; Hikosaka, Y.; Ito, K.; Motoki, S.; Yagishita, A. *Phys. Rev. Lett.* **2000**, *84*, 250–253.
- (19) Lin, P.; Lucchese, R. R. *J. Synch. Radiat.* **2001**, *8*, 150–153.
- (20) Glans, P.; Skytt, P.; Gunnelin, K.; Guo, J.-H.; Nordgren, J. *J. Electron Spectrosc. Relat. Phenom.* **1996**, *82*, 193–201.
- (21) Gel'mukhanov, F.; Ågren, H. *J. Phys. B* **1996**, *29*, 2751–2762.
- (22) Kempgens, B.; Köppel, H.; Kivimäki, A.; Neeb, M.; Cederbaum, L. S.; Bradshaw, A. M. *Phys. Rev. Lett.* **1997**, *79*, 3617–20.
- (23) Thomas, T. D.; Berrah, N.; Bozek, J.; Carroll, T. X.; Hahne, J.; Karlsen, T.; Kukuk, E.; Sæthre, L. J. *Phys. Rev. Lett.* **1999**, *82*, 1120–1123.
- (24) Petersen, H.; Senf, F.; Schäfers, F.; Bahrtdt, J. *Rev. Sci. Instrum.* **1995**, *66*, 1777–1779.
- (25) Senf, F.; Eggenstein, F.; Follath, R.; Hartlaub, S.; Lammert, H.; Noll, T.; Schmidt, J. S.; Reichardt, G.; Schwarzkopf, O.; Weiss, M.; Zeschke, T.; Gudat, W. *Nucl. Instrum. Methods A* **2001**, to be published.
- (26) Prince, K. C.; Vondráček, M.; Karvonen, J.; Coreno, M.; Camilloni, R.; Avaldi, L.; Simone, M. d. *J. Electron Spectrosc. Relat. Phenom.* **1999**, *101–103*, 141–147.
- (27) Mårtensson, N.; Baltzer, P.; Brühwiler, P. A.; Forsell, J.-O.; Nilsson, A.; Stenborg, A.; Wannberg, B. *J. Electron Spectrosc. Relat. Phenom.* **1994**, *70*, 117–128.
- (28) Baltzer, P.; Karlsson, L.; Lundqvist, M.; Wannberg, B. *Rev. Sci. Instrum.* **1993**, *64*, 2179–89.
- (29) Kuchiev, M. Y.; Sheinerman, S. A. *Soviet Physics–JETP* **1986**, *63*, 986–990.
- (30) Armen, G. B.; Tulkki, J.; Aberg, T.; Crasemann, B. *Phys. Rev. A* **1987**, *36*, 5606–5614.
- (31) Straten, P. v. d.; Morgenstern, R.; Niehaus, A. *Z. Phys. D* **1988**, *8*, 35–45.
- (32) Leclerc, G.; Pireaux, J. J. *J. Electron Spectrosc. Relat. Phenom.* **1995**, *71*, 141–164.
- (33) Cederbaum, L. S.; Domcke, W. *J. Chem. Phys.* **1976**, *64*, 603–611.
- (34) Carroll, T. X.; Hahne, J.; Thomas, T. D.; Sæthre, L. J.; Berrah, N.; Bozek, J.; Kukuk, E. *Phys. Rev. A* **2000**, *61*, 042503.
- (35) Cumpson, P. J.; Seah, M. P. *Surf. Interface Anal.* **1992**, *18*, 345–360.
- (36) Semenov, S. K.; Cherepkov, N. A., private communication.
- (37) Neeb, M.; Kivimäki, A.; Kempgens, B.; Köppe, H. M.; Feldhaus, J.; Bradshaw, A. M. *Phys. Rev. Lett.* **1996**, *76*, 2250–2253.
- (38) Neeb, M.; Kivimäki, A.; Kempgens, B.; Köppe, H. M.; Maier, K.; Bradshaw, A. M.; Kosugi, N. *Chem. Phys. Lett.* **2000**, *320*, 217–221.
- (39) Kempgens, B.; Köppe, H. M.; Kivimäki, A.; Neeb, M.; Maier, K.; Hergenhahn, U.; Bradshaw, A. M. *Phys. Rev. Lett.* **1997**, *79*, 35–38.
- (40) Lin, P.; Lucchese, R. R. *J. Chem. Phys.* **2000**, *113*, 1843–1851.
- (41) Kempgens, B.; Kivimäki, A.; Köppe, H. M.; Neeb, M.; Bradshaw, A. M.; Feldhaus, J. *J. Chem. Phys.* **1997**, *107*, 4219–4224.
- (42) Rennie, E. E.; Kempgens, B.; Köppe, H. M.; Hergenhahn, U.; Feldhaus, J.; Itchkawitz, B. S.; Kilcoyne, A. L. D.; Kivimäki, A.; Maier, K.; Piancastelli, M. N.; Polcik, M.; Rüdell, A.; Bradshaw, A. M. *J. Chem. Phys.* **2000**, *113*, 7362–7375.